European Conference on Computational Fluid Dynamics
ECCOMAS CFD 2006
P. Wesseling, E. Oñate and J. Périaux (Eds)

ADER SCHEMES FOR THE SHALLOW WATER EQUATIONS IN CHANNEL WITH IRREGULAR BOTTOM ELEVATION

G. Vignoli*, E.F. Toro† and V. Titarev†

*CISMA srl, c/o BIC Suedtirol
via Siemens, 19, 39100 Bolzano, Italy
e-mail: gianluca.vignoli@cisma.bz.it
web page: http://www.cisma.bz.it
†Laboratory of Applied Mathematics,
Department of Civil and Environmental Engineering, University of Trento,
via Mesiano, 77, 38050 Trento, Italy
e-mail: toro@ing.unitn.it, titarev@ing.unitn.it

Key words: High-order schemes; ADER; Well balanced, Derivative Riemann problem.

Abstract. *In this paper we develop one dimensional non-linear ADER schemes for the shallow water system with source terms. In contrast to conventional schemes we adopt a formulation given in terms of the free surface elevation and water discharge. Data reconstruction is performed using ENO polynomials both for the conservative variables and for the bottom elevation. The scheme is accurate up to forth order both in time and in space; essentially non-oscillatory results are obtained for discontinuous solutions both for the steady and unsteady case. The resulting numerical schemes can be applied to several realistic cases characterized by non-uniform geometries.*

1 INTRODUCTION

The one-dimensional shallow water equations have a wide range applications in open channel flows and river flows. In these cases source terms appear in the governing equations due to non-horizontal bed profile, bottom friction and variable channel width. A number of second-order Godunov-type schemes has been proposed to solve the shallow water with source terms (see [1,2]). The evaluation of the source term may require ad-hoc formulation, for example in [3] an upwind method is proposed for the treatment of the bed slope source term. In [4] data reconstruction is carried out in terms of the free surface elevation and a second order numerical scheme is developed which is able to reproduce both steady and unsteady solutions. This method is based on a particular data reconstruction of the free surface elevation, called the surface gradient method; moreover recostructed data are employed in a MUSCL-Handcock finite volume method with the HLL Riemann solver.

In this paper we propose an ADER scheme based on ENO[5] data reconstruction for the solution of the shallow water equations with a source term due to bottom slope. In order to obtain a well-balanced scheme the variables are given with respect to a staggered grid, as show in Figure 1. For the free surface elevation and water discharge the so-called cell-centred approach is adopted, while the bottom elevation is given at the cell interfaces.

The source term and the numerical fluxes are evaluated using the solution of the Derivative Riemann problem; the resulting numerical method is of arbitrary order of accuracy and reproduces smooth and discontinuous solutions, both steady and unsteady.

2 Formulation of the problem

The shallow water equations can be written in conservative form for the simple case of an horizontal bed channel and vanishing bottom friction. In the case of a shallow flow over a generic bed profile a source term in the governing equations appears (see [1,2]):

$$\begin{aligned} \frac{\partial D}{\partial t} + \frac{\partial Q}{\partial x} &= 0 \\ \frac{\partial Q}{\partial t} + \frac{\partial}{\partial x}\left(\frac{Q^2}{D} + \frac{1}{2}gD^2\right) &= -gD\frac{\partial b}{\partial x} \end{aligned} \tag{1}$$

where D is the flow depth, Q is the water discharge, $b(x)$ is the bottom elevation, t and x are time and the spatial independent variable respectively, g is the acceleration due to gravity.

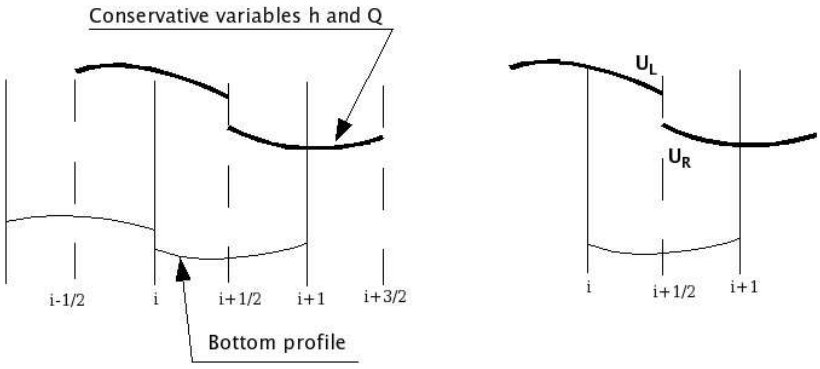

Figure 1: Formulation of the problem, (left) data reconstruction, (right) control volume and generalized Riemann problem.

In the case of equations with source terms standard numerical schemes do not perform satisfactory, particulary for the steady case. We note that in the literature regarding well-balanced schemes there are two different definitions of steady flow, the first consists in vanishing velocities everywhere in the computational domain, the second refers to the case of steady solution with non vanishing velocities. Standard explicit schemes for the

shallow water with source terms do not converge to the exact solution also in the first case.

In order to design a numerical method able to reproduce both steady and unsteady solutions we follow [4] and propose a formulation, given in term of the free surface elevation $h = D + b$. Using this notation system (1) becomes:

$$\begin{aligned} \frac{\partial h}{\partial t} + \frac{\partial Q}{\partial x} &= 0 \\ \frac{\partial Q}{\partial t} + \frac{\partial}{\partial x}\left(\frac{Q^2}{h-b} + \frac{1}{2}gh^2 - gbh\right) &= -gh\frac{\partial b}{\partial x} \end{aligned} \tag{2}$$

System (2) is hyperbolic with eigenvalues $\lambda^{(i)}$ and right eigenvectors $R^{(i)}$:

$$\lambda^{(1)} = u - a,\ \lambda^{(2)} = u + a$$

$$\mathbf{R}^{(1)} = \begin{pmatrix} 1 \\ u-a \end{pmatrix}, \quad \mathbf{R}^{(2)} = \begin{pmatrix} 1 \\ u+a \end{pmatrix}$$

where $u = Q/D$ is the flow velocity and $a = \sqrt{gD}$ is the celerity.

The two main advantages of the formulation (2) are that the model reproduces in the right way the physics of the problem, and it is possible to use the well known exact Riemann solver proposed by [6] in order to evaluate the numerical fluxes between disjoint computational volumes.

3 Numerical scheme

System (2) can be written in the following conservative form:

$$\frac{\partial \mathbf{U}}{\partial t} + \frac{\partial \mathbf{F}}{\partial x} = \mathbf{S} \tag{3}$$

where the unknown vector $\mathbf{U}$, the flux vector $\mathbf{F}$ and the source term S are given by

$$\mathbf{U} = \begin{pmatrix} h \\ Q \end{pmatrix}, \quad \mathbf{F} = \begin{pmatrix} Q \\ \frac{Q^2}{h-b} + \frac{1}{2}gh^2 - ghb \end{pmatrix}, \quad S = \begin{pmatrix} 0 \\ -gh\frac{\partial b}{\partial x} \end{pmatrix}.$$

Integration of (3) over the control volume $I_i = \left[x_{i-\frac{1}{2}}, x_{i+\frac{1}{2}}\right]$ in the $x-t$ plane $I_i \mathrm{x} \Delta t$ gives:

$$\mathbf{U_i^{n+1}} = \mathbf{U_i^n} - \frac{\Delta t}{\Delta x}\left(\mathbf{F_{i+\frac{1}{2}}} - \mathbf{F_{i-\frac{1}{2}}}\right) + \Delta t \mathbf{S_i} \tag{4}$$

Here the cell average of the solution $\mathbf{U_i^n}$ at time level t^n, the time average of the flux $\mathbf{F_{i+\frac{1}{2}}}$ at cell interface $x_{i+\frac{1}{2}}$, time-space average of the source term $\mathbf{S_i}$ over the control volume

are given by

$$\mathbf{U_i^n} = \frac{1}{\Delta x}\int_{x_{i-\frac{1}{2}}}^{x_{i+\frac{1}{2}}} \mathbf{U}\left(t^n, x\right) dx, \quad \mathbf{F_{i+\frac{1}{2}}} = \frac{1}{\Delta t}\int_{t^n}^{t^n+\Delta t} \mathbf{F}\left(x_{i+\frac{1}{2}}, t\right) dt,$$

$$\mathbf{S_i} = \frac{1}{\Delta t \Delta x}\int_{t^n}^{t^n+\Delta t}\int_{x_{i-\frac{1}{2}}}^{x_{i+\frac{1}{2}}} \mathbf{S}\left(x, t\right) dx dt.$$

Equation (4) involving integral averages is an exact relation, but can be used to construct numerical methods to compute approximate solutions to (3). In order to solve (3) numerically the computational domain is divided into many disjoint control volumes. Then approximate numerical fluxes and approximate numerical source are defined and denoted by the same symbols $\mathbf{F_{i+\frac{1}{2}}}$ and $\mathbf{S_i}$ then equation (4) is a conservative one step scheme to solve (3).

In order to construct a numerical method for the solution of (3) we use the so called cell centred approach for the unknown vector $\mathbf{U}$. The bottom elevation, which appears only in the formulation for the fluxes $\mathbf{F_{i+\frac{1}{2}}}$, is given using the interface centered approach; the averaged values $b_{i+\frac{1}{2}}$ are defined as

$$b_{i+\frac{1}{2}} = \int_{x_i}^{x_{i+1}} b\left(x\right) dx.$$

In order to develop high order numerical schemes we use the ADER methods for the evaluation of the numerical fluxes and of the numerical source term. This approach consists of a suitable definition of both $\mathbf{F_{i+\frac{1}{2}}}$ and $\mathbf{S}_i$ in such a way that the resulting numerical solution is of arbitrary high order of accuracy both in time and in space. By the order of accuracy of the numerical scheme we mean the convergence rate of the numerical solution to the exact solution when the mesh is refined with a fixed Courant number.

The ADER approach consists in three steps:

1. reconstruction of the pointwise values of the solution starting from the cell averages;
2. solution of the derivative Riemann problem and evaluation of the intercell fluxes $\mathbf{F_{i+\frac{1}{2}}}$;
3. evaluation of the numerical source $\mathbf{S}_i$ by integrating a time-space Taylor expansion of the solution inside the control volume.

The point wise values of the solution at time level t^n are evaluated from the cell averages using high order polynomials. In this paper we use the ENO[5] reconstruction procedure in order to avoid spurious oscillations, leading to a non-linear numerical scheme. We note that the reconstruction is performed both for the unknown vector $\mathbf{U}$ and for the bottom elevation b, as shown in figure 1.

After the data reconstruction we solve the following Derivative Riemann problem:

$$\partial_t \mathbf{U} + \partial_x \mathbf{F}(\mathbf{U}) = \mathbf{S}(\mathbf{U}),$$
$$\mathbf{U}(x,0) = \begin{cases} \mathbf{U}_L(x) = \mathbf{p}_i(x), & x < x_{i+\frac{1}{2}}, \\ \mathbf{U}_R(x) = \mathbf{p}_{i+1}(x), & x > x_{i+\frac{1}{2}} \end{cases} \tag{5}$$

where $\mathbf{p}_i(x)$ denotes the reconstructed polynomial in the i-th cell. Please note that the value $b_{i+\frac{1}{2}}$ as well as its spatial derivative are known.

Following [7] we find the approximate flux at cell interface using an appropriate Gaussian rule:

$$\mathbf{F}_{i+\frac{1}{2}} = \sum_{\alpha=0}^{N} \mathbf{F}\left(\mathbf{U}_{i+\frac{1}{2}}(\gamma_\alpha \Delta t)\right) K_\alpha \tag{6}$$

where γ_α are suitable Gaussian coefficients. The vector $\mathbf{U}_{i+\frac{1}{2}}(\tau)$ is the solution of the DRP problem (5) which is expressed as a Taylor expansion:

$$\mathbf{U}_{i+\frac{1}{2}}(\tau) = \mathbf{U}_{i+\frac{1}{2}}\left(0^+\right) + \sum_{k=1}^{r-1}\left[\partial_t^{(k)}\mathbf{U}_{i+\frac{1}{2}}\left(0^+\right)\frac{\tau^k}{k!}\right], \quad \partial_t^{(k)}\mathbf{U}_{i+\frac{1}{2}}\left(0^+\right) = \frac{\partial^k}{\partial t^k}\mathbf{U}_{i+\frac{1}{2}}\left(0^+\right). \tag{7}$$

where $0^+ = \lim_{t\to 0^+} t$. The leading term $\mathbf{U}_{i+\frac{1}{2}}(0^+)$ can be evaluated once the boundary extrapolated values $\mathbf{U}_L\left(x_{i+\frac{1}{2}}\right)$ and $\mathbf{U}_R\left(x_{i+\frac{1}{2}}\right)$ are known, by the solution of conventional Riemann problem with piecewise constant data:

$$\partial_t \mathbf{U} + \partial_x \mathbf{F}(\mathbf{U}) = 0$$
$$\mathbf{U}(x,0) = \begin{cases} \mathbf{U}_L\left(x_{i+\frac{1}{2}}\right), & x < x_{i+\frac{1}{2}} \\ \mathbf{U}_R\left(x_{i+\frac{1}{2}}\right), & x > x_{i+\frac{1}{2}} \end{cases}$$

evaluated for $\left(x - x_{i+\frac{1}{2}}\right)/t = 0$. We call $\mathbf{U}_{i+\frac{1}{2}}(0^+)$ the Godunov state, which in this paper is evaluated using the exact Riemann solver[6]. The remaining terms in (7) are computed by replacing all time derivatives $\partial_t^{(k)}\mathbf{U}_{i+\frac{1}{2}}(0^+)$ by spatial derivatives $\partial_x^{(k)}\mathbf{U}_{i+\frac{1}{2}}(0^+)$ by means of the Cauchy-Kowalesky procedure. The unknown spatial derivatives at $t = 0+$ are found from the following linearised Riemann problems:

$$\partial_t\left(\partial_x^{(k)}\mathbf{U}\right) + A\left(\mathbf{U}_{i+\frac{1}{2}}\left(0^+\right)\right)\partial_x\left(\partial_x^{(k)}\mathbf{U}\right) = 0$$
$$\partial_x^{(k)}\mathbf{U}(x,0) = \begin{cases} \partial_x^{(k)}\mathbf{U}_L\left(x_{i+\frac{1}{2}}\right), & x < x_{i+\frac{1}{2}}, \\ \partial_x^{(k)}\mathbf{U}_R\left(x_{i+\frac{1}{2}}\right), & x > x_{i+\frac{1}{2}} \end{cases}$$

where the matrix $A\left(\mathbf{U}_{i+\frac{1}{2}}(0^+)\right)$ is reported in Appendix. The boundary extrapolated values $\partial_x^{(k)}\mathbf{U}_L\left(x_{i+\frac{1}{2}}\right)$ and $\partial_x^{(k)}\mathbf{U}_R\left(x_{i+\frac{1}{2}}\right)$ are evaluated using the polynomials $p_i(x)$, $p_{i+1}(x)$ obtained by the ENO reconstruction procedure.

To evaluate the source term we perform integration by parts:

$$\begin{aligned}\Delta t\Delta x\mathbf{S}_i &= \int_0^{\Delta t}\int_{x_{i-\frac{1}{2}}}^{x_{i+\frac{1}{2}}}\left(-gh\frac{\partial b}{\partial x}\right)dxdt = \\ &= -g\int_0^{\Delta t}\left(hb|_{x_{i+\frac{1}{2}}} - hb|_{x_{i-\frac{1}{2}}}\right)dt + g\int_0^{\Delta t}\int_{x_{i-\frac{1}{2}}}^{x_{i+\frac{1}{2}}} b\frac{\partial h}{\partial x}dxdt\end{aligned} \tag{8}$$

The first integral is evaluated using suitable Gaussian point and the Taylor expansion of the interface state in time (10). The second integral in (8) is approximated by a Gaussian integration rule:

$$g\int_0^{\Delta t}\int_{x_{i-\frac{1}{2}}}^{x_{i+\frac{1}{2}}} b\frac{\partial h}{\partial x}dxdt = g\sum_{\alpha=1}^{N}\left[\sum_{l=1}^{N}\left(b(x_\alpha)\frac{\partial}{\partial x}h(x_\alpha,\tau_l)\right)K_l\right]K_\alpha. \tag{9}$$

3.1 Riemann solver for the linearised equations

The ADER approach requires the solution of several linearised Riemann problem for the space derivatives of the unknowns h and Q. The linear Riemann problem to be solved for any order of spatial derivative has the same structure as the homogeneous linearised problem for the unknowns h and Q:

$$\begin{aligned}\frac{\partial h}{\partial t} + \frac{\partial Q}{\partial x} &= 0,\\ \frac{\partial Q}{\partial t} + \left(gD - u^2\right)\frac{\partial h}{\partial x} + 2u\frac{\partial Q}{\partial x} &= 0.\end{aligned} \tag{10}$$

For simplicity here we report the solution h^* and Q^* for (10); it is easy to obtain linear solutions for all the space derivatives involved in the ADER expansion substituting h by $\frac{\partial^n h}{\partial x^n}$ and Q by $\frac{\partial^n Q}{\partial x^n}$. Please refer to [6] for further details on the solution procedure, here we report the final results:

$$\begin{pmatrix} h^* \\ Q^* \end{pmatrix} = \begin{cases} \begin{pmatrix} h_L \\ Q_L \end{pmatrix}, & \lambda^+,\lambda^- > 0 \\ \begin{pmatrix} \frac{h_R+h_L}{2} + \frac{1}{2a}\left[u\left(h_R-h_L\right) - \left(Q_R-Q_L\right)\right] \\ \frac{Q_R+Q_L}{2} - \frac{a}{2}\left(h_R-h_L\right) - \frac{1}{2a}\left[u\left(Q_R-Q_L\right) - u^2\left(h_R-h_L\right)\right] \end{pmatrix}, & \begin{matrix}\lambda^+ > 0,\\ \lambda^- < 0\end{matrix} \\ \begin{pmatrix} h_R \\ Q_R \end{pmatrix}, & \lambda^+,\lambda^- < 0 \end{cases}$$

4 Numerical tests

4.1 Steady solution

Following [1,2,3] and [4] the first numerical test is the fully steady test. In such condition the proposed model reproduces exactly the horizontal free surface elevation and zero velocity in the whole numerical domain.

The test under steady condition is more interesting sincen there are several different configuration characterized by smooth or discontinuous solutions, depending on the values of the parameters, namely the channel discharge Q, the boundary conditions for the free surface elevation $h\left(x=0\right)$ and $h\left(x=L\right)$, where L is the channel length and the maximum height of the bed profile b_{max}. Figures 2 and 3 show the numerical results of the standard test case of a subcritical flow over a parabolic bump.

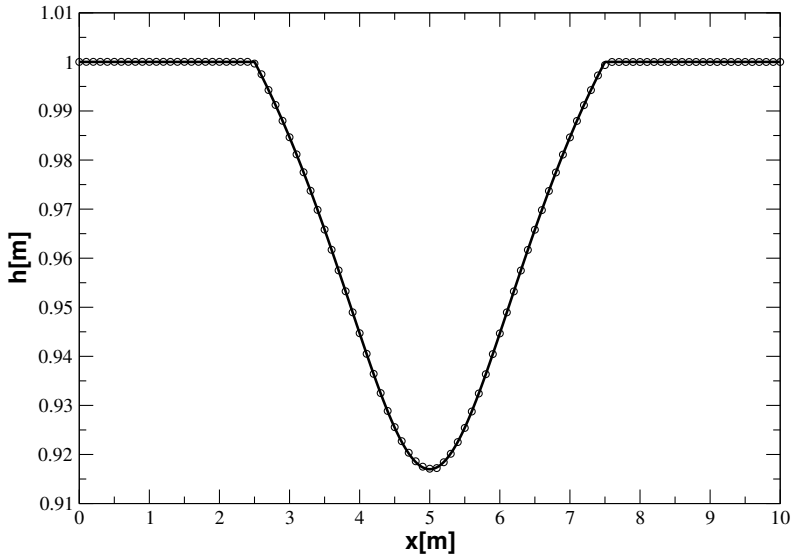

Figure 2: Free surface elevation in the case of smooth solution and parabolic bed profile, ADER2 numerical method. ($Q = 1m^3/s$, $b_{max} = 0.3m$, $h\left(x=L\right) = 1m$, $N = 100$, $L = 10m$)

Figures 4 and 5 show the numerical solution for the flow over a parabolic bump with a stationary shock. We note that the numerical solution reproduces well both the free surface elevation and the discharge. For this test problem we note that the position of the shock is stationary and depends on the discharge, the maximum bottom elevation and on the boundary conditions. We remark that it is possible to obtain an accurate numerical solution as plotted in Figure 4 if we choose the spatial mesh in such a way that the shock is positioned exactly between two numerical cells, in this case $N = 280$. Please note that this procedure is not general because the position of the shock is not known *a priori*. In other words, for the steady shock solution the refinement of the computational grid does not always give more accurate results, as can be seen from Figure 4.

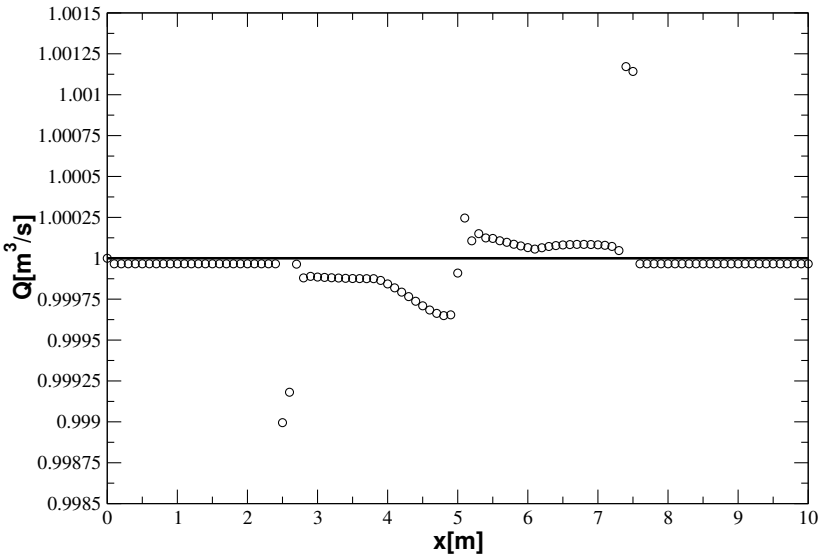

Figure 3: Discharge in the case of smooth solution and parabolic bed profile, ADER2 numerical method. ($Q = 1m^3/s$, $b_{max} = 0.3m$, $h\,(x = L) = 1m$, $N = 100$, $L = 10m$)

4.2 Unsteady solution

Unfortunately, the unsteady reference solution for free surface water flows over a complex topography is not available. Figure 6 shows the results for the standard test problem of a dam break over a horizontal bed. We see that essentially non-oscillatory results are obtained.

In figure 7 is reported an example of a dam break problem over a Gaussian bed profile; under these conditions the solution displays two different shocks. The fist one is due to the initial condition; the appears in the middle region of the flow due to the bottom slope. The first shock propagates landward faster than the second, which is *quasi* stationary.

5 Density convergence test

5.1 Steady case

In order to evaluate the order of accuracy of the scheme we perform numerical tests with a smooth bed profile, e.g.e a Gaussian or sinusoidal bottom profile. The maximum bed elevation is chosen small enough such that the resulting solution does not have discontinuities of the free surface elevation. The mesh convergence study has been made using both Gaussian and sinusoidal bed profiles for a fixed Courant number. For the sinusoidal bed profile results are in agreement with the designed order of accuracy of the

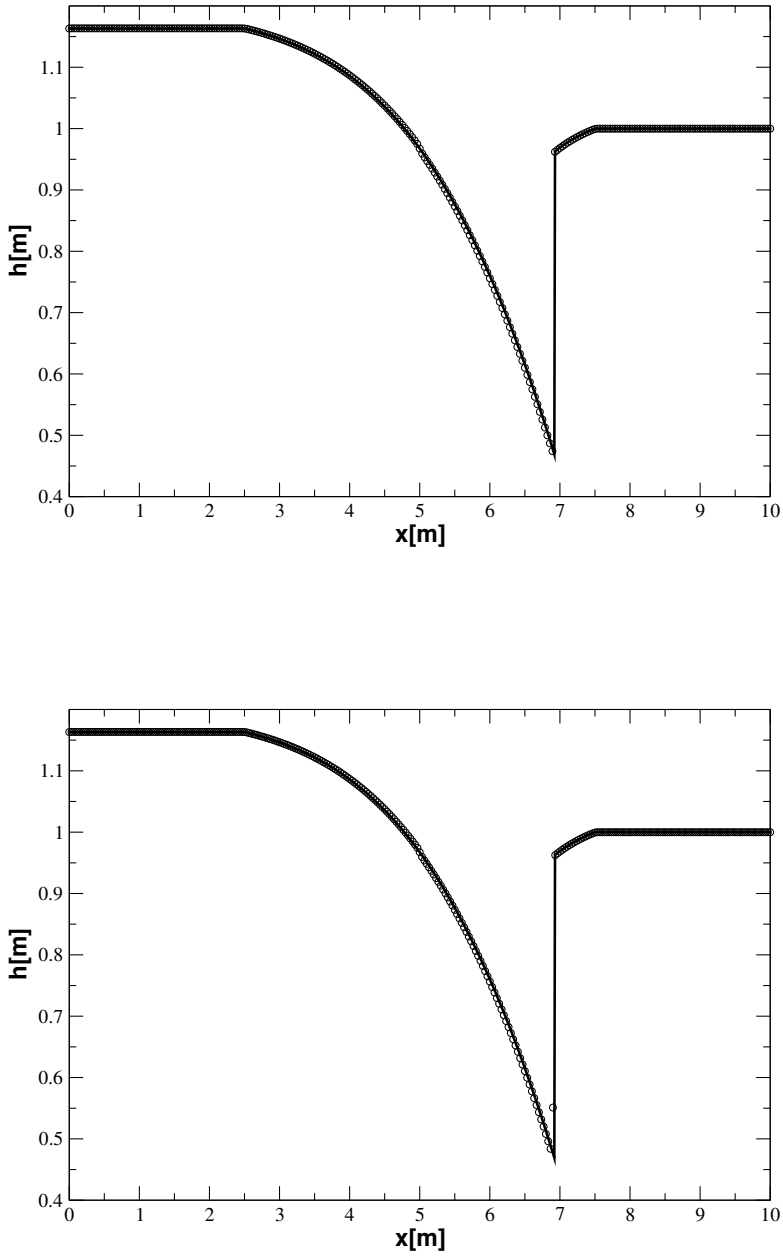

Figure 4: Free surface elevation in the case of discontinuous solution and parabolic bed profile, ADER2 numerical method. ($Q = 1m^3/s$, $b_{max} = 0.5m$, $h\,(x = L) = 1m$, top $N = 280$, bottom $N = 300$, $L = 10m$)

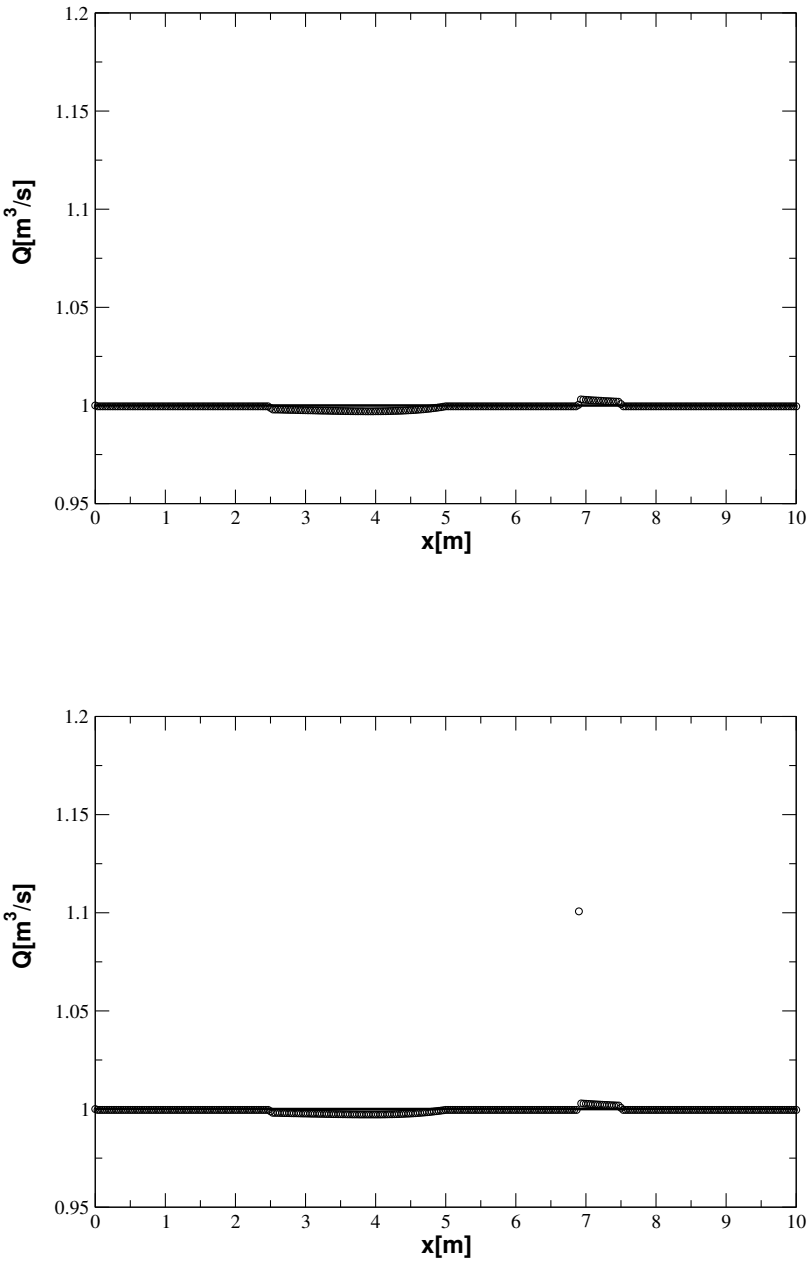

Figure 5: Discharge elevation in the case of discontinuous solution and parabolic bed profile, ADER2 numerical method. ($Q = 1m^3/s$, $b_{max} = 0.5m$, $h\,(x = L) = 1m$, top $N = 280$, bottom $N = 300$, $L = 10m$)

numerical scheme whereas for the Gaussian bed profile the achieved order of accuracy does not match the designed one, in particular for the ADER4 scheme. As expected, the forth-order scheme is the most accurate scheme.

Method	N	L_1 error	L_1 order	L_∞ error	L_∞ order
ADER2	5	0.1171E-02		0.2484E-02	
	10	0.2802E-03	2.063	0.6061E-03	2.035
	20	0.6173E-04	2.182	0.1361E-03	2.154
	40	0.1467E-04	2.072	0.3096E-04	2.136
	80	0.3583E-05	2.034	0.7296E-05	2.085
ADER 3	5	0.4894E-03		0.1113E-02	
	10	0.7690E-04	2.669	0.1488E-03	2.902
	20	0.9915E-05	2.955	0.2004E-04	2.892
	40	0.1288E-05	2.944	0.2565E-05	2.965
	80	0.1645E-06	2.969	0.3234E-06	2.987
ADER 4	5	0.3025E-03		0.6851E-03	
	10	0.1914E-04	3.982	0.4409E-04	3.957
	20	0.1193E-05	4.003	0.2924E-05	3.914
	40	0.7200E-07	4.051	0.2230E-06	3.712
	80	0.9164E-08	2.973	0.2621E-07	3.089

Table 1: Density convergence test for the steady and smooth case, sinusoidal bed profile ($b_{max} = 0.01m$, $Q = 1m^3s^{-1}$, $h\,(x = L) = 1m$, Courant number=0.9)

5.2 Unsteady case

The unsteady flow test has been constructed by adding an additional source term to the momentum equation so that the time dependent sinusoidal solutions for the free surface and for the discharge over a sinusoidal bed profile are obtained:

$$h = h_0 + a_0 \sin\left(2\pi\frac{x}{L}\right)\cos\left(2\pi\frac{t}{T_0}\right) \tag{11}$$

$$Q = Q_0 - \frac{a_0 L}{T_0}\cos\left(2\pi\frac{x}{L}\right)\sin\left(2\pi\frac{t}{T_0}\right) \tag{12}$$

$$b = b_0 \sin\left(2\pi\frac{x}{L}\right). \tag{13}$$

where L is the longitudinal extension of the computational domain and T_0 a suitable time period. The new source term has been evaluated numerically by using Gaussian integration over the control volume.

Method	N	L_1 error	L_1 order	L_∞ error	L_∞
ADER2	5	0.3570E-04		0.9711E-04	
	10	0.1171E-04	1.607	0.2866E-04	1.760
	20	0.3045E-05	1.943	0.8188E-05	1.807
	40	0.7605E-06	2.001	0.2121E-05	1.948
	80	0.1893E-06	2.006	0.5428E-06	1.966
ADER3	5	0.2499E-04		0.7595E-04	
	10	0.3862E-05	2.693	0.8526E-05	3.155
	20	0.5508E-06	2.809	0.1144E-05	2.897
	40	0.7646E-07	2.848	0.1712E-06	2.740
	80	0.1046E-07	2.868	0.3375E-07	2.342
ADER4	5	0.1607E-04		0.4548E-04	
	10	0.1969E-05	3.028	0.4682E-05	3.279
	20	0.3078E-06	2.677	0.1901E-05	1.300
	40	0.4470E-07	2.783	0.2685E-06	2.823
	80	0.5129E-08	3.123	0.4873E-07	2.462

Table 2: Density convergence test for the steady and smooth case, Gaussian bed profile ($b_{max} = 0.001m$, $Q = 1m^3s^{-1}$, $h\,(x = L) = 1m$, Courant number=0.9)

Method	N	L_1 error	L_1 order	L_∞ error	L_∞
ADER 2	5	0.1520E-02		0.3328E-02	
	10	0.3891E-03	1.965	0.7958E-03	2.064
	20	0.8029E-04	2.276	0.1807E-03	2.138
	40	0.1816E-04	2.143	0.4053E-04	2.156
	80	0.4337E-05	2.066	0.9466E-05	2.098
ADER 3	5	0.6630E-03		0.1258E-02	
	10	0.6481E-04	3.354	0.1493E-03	3.074
	20	0.1023E-04	2.662	0.2106E-04	2.826
	40	0.1322E-05	2.952	0.2712E-05	2.957
	80	0.1647E-06	3.005	0.3415E-06	2.989
ADER 4	5	0.3720E-03		0.8252E-03	
	10	0.2775E-04	3.744	0.5868E-04	3.813
	20	0.1438E-05	4.270	0.3117E-05	4.234
	40	0.8418E-07	4.094	0.2151E-06	3.856
	80	0.1085E-07	2.955	0.2237E-07	3.265

Table 3: Density convergence test for the unsteady and smooth case after $t = 400s$, ($b_{max} = 0.01m$, $a_0 = 0.01m$, $Q_0 = 1m^3/s$, $T_0 = 10000s$, Courant number=0.9)

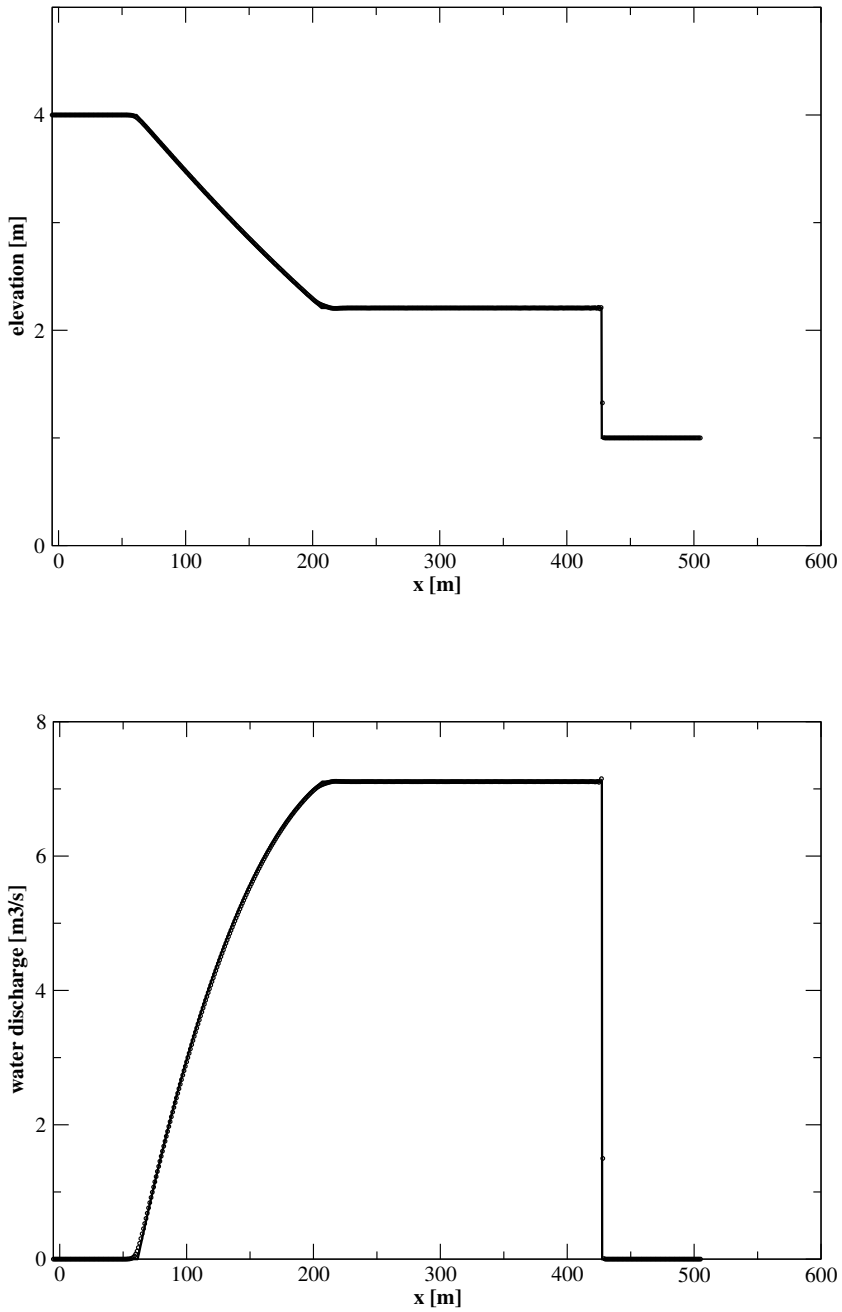

Figure 6: Dam break over a horizontal bed profile. ADER3 numerical scheme; $t = 30s$, Courant number=0.9, $N = 500$.

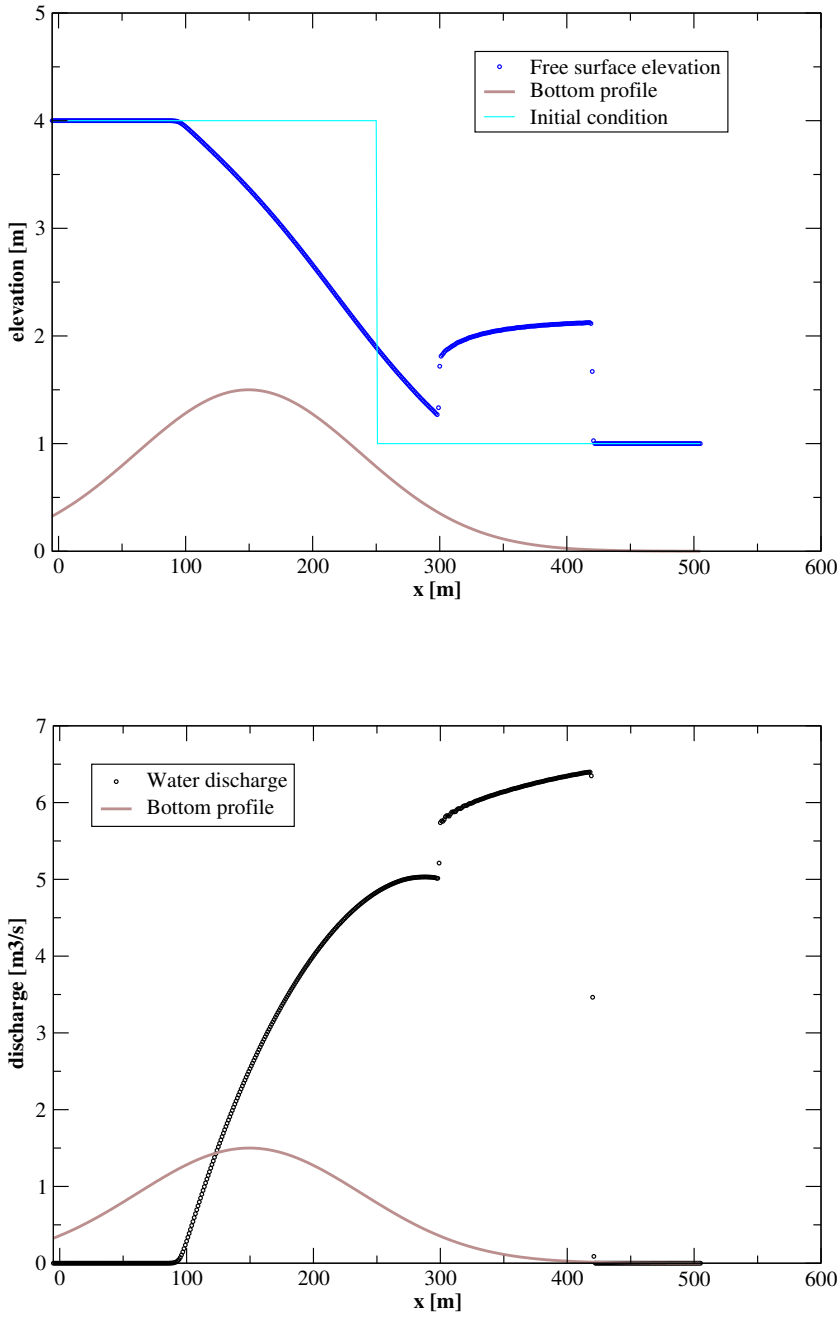

Figure 7: Dam break over a non horizontal profile. ADER3 numerical scheme. The solution displays two shocks, both propagating landward, but with different celerities; $t = 40s$, Courant number=0.9, $N = 500$.

6 Conclusions

We have proposed a framework for constructing arbitrary high order numerical schemes for the solution of the shallow water equations with source term. The numerical method reproduces the steady solution (horizontal free surface elevation and vanishing velocities) without spurious oscillations.

Steady solutions are also well reproduced both in the smooth and in the discontinuous case. Moreover we have shown that in the case of steady discontinuous solution a refinement of the grid does not always give better numerical solution around discontinuities. In this case better solutions are obtained when one cell interface is aligned with the discontinuity.

The numerical method reproduces also unsteady solution and essentially non-oscillatory results are obtained.

Acknowledgements. The first and thid authors acknowledge the financial support provided by the PRIN programme (2004-2006) of Italian Ministry of Education and Research (MIUR).

REFERENCES

[1] Maria Elena Vazquez-Cendon. Improved treatment of source terms in upwind schemes for the shallow water equations in channels with irregular geometry. *Journal of Computational Physics*, **148**, 497–526, (1999).

[2] P. Garcia-Navarro, F. Alcrudo, and J. M. Saviron. 1d open channel flow simulation using TVD Maccormack. *J. Hydraulic Eng., ASCE*, **118(10)**, 1359–1372, (1992).

[3] A. Bermudez and M. E. Vazquez Upwind Methods for Hyperbolic Conservation Laws with Source Terms. *Comput. Fluids*, **23(8)**, 1049–1071, (1994).

[4] J. G. Zhou, D. M. Causon, C. G. Mingham, and D. M. Ingram. The surface gradient method for the treatment of source terms in the shallow-water equations. *Journal of Computational Physics*, **168**, 1–25, (2001).

[5] C.-W. Shu. Essentially Non-Oscillatory and Weighted Essentially Non-Oscillatory Schemes for Hyperbolic Conservation Laws. NASA CR-97-206253 ICASE Report No. 97-65, Institute for Computer Applications in Science and Engineering, NASA Langley Research Center Hampton, (1997).

[6] E. F. Toro. *Shock-Capturing Methods for Free-Surface Shallow Flows* Wiley and Sons Ltd., (2001).

[7] E.F. Toro and V.A. Titarev. ADER schemes for scalar non-linear hyperbolic conservation laws with source terms in three-space dimensions. *Journal of Computational Physics*, **202**, 196–215, (2005).